J Arid Land (2023) 15(5): 578–601
https://doi.org/10.1007/s40333-023-0012-9

Science Press Springer-Verlag

Fate of rubber bush (*Calotropis procera* (Aiton) W. T. Aiton) in adversary environment modulated by microstructural and functional attributes

Ummar IQBAL[1*], Mansoor HAMEED[2], Farooq AHMAD[2], Muhammad S AAHMAD[2], Muhammad ASHRAF[2]

[1] Department of Botany, the Islamia University of Bahawalpur, Bahawalpurwala 64200, Pakistan;
[2] Department of Botany, University of Agriculture, Faisalabad 38040, Pakistan

Abstract: *Calotropis procera* (Aiton) W. T. Aiton, belonging to the family Apocynaceae, is C_3 evergreen plant species in arid and semi-arid areas of the Punjab Province, Pakistan. It grows in a variety of habitats like salt affected and waterlogged area, desert/semi-desert, roadside, wasteland, graveyard, forest, crop field, coastline, and river/canal bank. A total of 12 populations growing in different ecological regions were sampled to evaluate their growth, physio-biochemical, and anatomical responses to specific environmental condition. Population adapted to desert/semi-desert showed vigorous growth (plant height, shoot length, and number of leaves), enhanced photosynthetic level (chlorophyll *a*, chlorophyll *b*, carotenoids, and total chlorophyll), and apparent anatomical modifications such as increased stem radius, cuticle thickness, storage parenchyma tissues (cortex and pith), and vascular bundles in stems, while the maximum of midrib and lamina thickness, epidermal cells, cuticle thickness, cortical proportion, abaxial stomatal density, and its area in leaves. There was high plasticity in structural and functional features of these populations, which enable them to survive and tolerate under such hot and dry desert environment. Population of saline areas exhibited very critical modifications to sustain under salt prone environment. At physiological level, it possesses the maximum amount of organic osmolytes (glycine betaine and proline) and antioxidants (superoxide dismutase (SOD), catalase (CAT), and peroxidase (POD)), while at anatomical level, it showed intensive sclerification, large phloem region (inner and outer), pith parenchyma cells, and metaxylem vessels in stems and leaves. The population of dry mountains showed very distinctive features, such as increased shoot ionic contents (K^+ and Ca^{2+}), collenchyma and sclerenchyma thickness in stems, trichomes size, and numerous small stomata on abaxial surface of leaves. It is concluded that no definite or precise single character can be taken as a yardstick for adjudging the biomass production in this rubber bush weed population.

Keywords: *Calotropis procera*; Apocynaceae; phenotypic plasticity; aridity; rubber bush

Citation: Ummar IQBAL, Mansoor HAMEED, Farooq AHMAD, Muhammad S AAHMAD, Muhammad ASHRAF. 2023. Fate of rubber bush (*Calotropis procera* (Aiton) W. T. Aiton) in adversary environment modulated by microstructural and functional attributes. Journal of Arid Land, 15(5): 578–601. https://doi.org/10.1007/s40333-023-0012-9

1 Introduction

Calotropis procera is drought resistant and salt tolerant xerophytic C_3 plant, widely growing in arid and semi-arid areas. It can grow in a variety of habitats like high salinity, waterlogging, desert/semi-desert, river/canal bank, coastline, forest, railway tract, wasteland, open and barren

*Corresponding author: Ummar IQBAL (E-mail: ummariqbal@yahoo.com)
Received 2022-11-24; revised 2023-02-20; accepted 2023-03-13

fields, and roadside. It keeps evergreen under open field condition from young vegetative stage to mature reproductive stage (Boutraa, 2010; Menge et al., 2016). In the Punjab Province of Pakistan, the plant shows a wider geographically distribution and invades different habitats. However, the mechanism involving in successful distribution of this species across heterogenic environments are still unexplored. In this scenario, a comprehensive research was implemented to investigate the responses of populations specific to environmental condition.

Rapid increase in ambient CO_2 concentration and temperature fluctuation of the planet is causing global climatic change along with significant alteration in seasonal precipitation, and ultimately leading to aridity towards less or semi-arid areas of the world (Koutroulis, 2019). High temperature and dry environment are two main factors that strongly influence the success and rehabilitation of plant communities. By understanding the survival mechanism of these plant communities, we could improve the protection of natural vegetation of these areas (Peñuelas et al., 2018). As in most of the terrestrial environments, water availability is considered as major limiting factor for photosynthesis, growth, and productivity, even in plants thrive well under arid conditions, and influences the population dynamics (Duan et al., 2018).

Abiotic stresses (drought and salinity) impose harmful impacts on plant growth through various means such as physiological drought condition upon restricted supply of water under osmotic stress, disruption of cellular functions, and physiological process like photosynthesis and respiration through ionic imbalance or toxicity (Muhammad et al., 2021). Ultimately, it causes ROS (reactive oxygen species) accumulation in metabolically active sites, which may impair the biological structure and its process (Sachdev et al., 2021). For example, superoxide radicle, hydrogen peroxide, singlet oxygen, and hydroxyl radical are generated in cell, which perturb the biochemical events by disrupting membranous organelles and metabolites (Ahanger et al., 2017). In counteract of such oxidants plants produce enzymatic and non-enzymatic antioxidants. The most vital enzymatic antioxidants are peroxidase (POX), superoxide dismutase (SOD), and catalase (CAT), while non-enzymatic antioxidants included carotenoids, polyphenols, glutathione, ascorbate, tocopherols, anthocyanins, etc., which scavenge the most of ROS molecules (Batool et al., 2013).

Seasonal falling of leaves, smallest thicker leaves, surface pubescence, organ succulence, epidermal and cuticle thickness, lignification of mechanical tissues, and small and fewer stomata that are oriented in crypts or abaxial leaf surfaces (Abd Elhalim et al., 2016), extensive root system, and greater water use efficiency are the main adaptations of arid plant communities (Fatima et al., 2021). All of these features are specific to minimize the transpirational loss, mainly by leaf surface, which is crucial strategy for water conservation. Reduction in vessels diameter is another key feature that may affect water conduction, but it minimizes the risk of embolism or cavitation (Kaleem and Hameed, 2021).

C. procera (Apocynaceae) commonly known as giant milk weed, rubber bush is a perennial and woody, 3–5 m long evergreen shrub. It has silver green leaves, opposite and sub-sessile, purple-tipped flowers, and inflated pale green seed pods (Rivas et al., 2020). It is native to tropical and sub-tropical regions of Asia and Africa, and commonly found in the Middle East. It grows as wasteland plant and reproduces by seeds only. It shows vigorous growth under adverse climate and poor soil condition (Pompelli et al., 2019). It can withstand drought and salt affected environment, but the mechanism behind their success in arid and semi-arid areas is totally unclear. It quickly colonizes a variety of habitats like roadside, stream/river bank, lagoon edge, and overgrazed area via different phenomena like anemochory and zoochory. It dominates the areas of sandy soil with low rainfall, and considered to be indicator of degraded lands. It attracts and supports 80% wildlife for completion of their life cycle (Khan et al., 2019).

Although this species has great ecological importance as it supports the several wild species like pollinators, i.e., honeybees, ants, butterflies, and casual visitors like wasp, moths and dragonfly in such open fields and deserted environments, and it might be one of major causes of their wide distributional ranges. But this is not enough criteria to judge the potential of species survival in the variety of habitats, there would be some alteration at growth, structural, and

functional levels in response to different environmental stresses, which determine their ecological success across heterogenic environments. In this scenario, this work aims to answer the following questions: (1) are morpho-anatomical and physiological traits of *C. procera* plastic in nature? (2) whether this species modifies its structural and functional features according to the environmental conditions? and (3) what are the traits that determine the ecological success of the species? This study was carried out to evaluate the structural and functional mechanism of different populations of *C. procera*, and relating its adaptive features to environment, which enables them to colonize a variety of habitats especially in arid or semi-arid areas of the Punjab Province, Pakistan. It was hypothesized that this species must adopt internal (anatomical) and external (morphological) mechanisms to cope with prevailing environmental conditions. Such adaptive components can be extracted and incorporated as biological markers into sensitive species to revegetate the wasteland of these areas.

2 Materials and methods

2.1 Climatic condition of the Punjab Province

The environmental condition of the Punjab Province ranges from tropical to sub-tropical, arid to semi-arid, dry, and hot. Average annual precipitation of the province fluctuates from 250 to 1000 mm, the maximum precipitation was in the monsoon season (June–August). The northern hilly areas receive more annual precipitation (1000 mm) as compared with southern plain areas that receive less than 250 mm precipitation. The maximum average temperature of a region is 48°C in June and the minimum is 4°C in January (Pakistan Meteorological Department). Coordinates and altitudes of sampling sites were recorded with the help of the global positioning system.

2.2 Plant material selection

Each study site was explored in an area of 1 km^2 for tagging the plants of each population. Six largest plants (replications; n=6) were subjectively selected at each collection site (habitat) keeping the plant distance at least 5 m. Sampling method was a single plant per replication from each population. Sampling points were randomly selected within each population. Sampling was done during August–October 2020. The youngest shoot was selected for anatomical studies.

2.3 Study layout, soil topography, and coordinates

This study was carried out under natural conditions (semi-arid and arid areas) in the Punjab Province of Pakistan, where *C. procera* populations were found. A total 12 populations from heterogenic environments were collected to evaluate their structural and functional responses (Fig. 1). The selected regions varied by their geographical conditions, habitats, and soil types. These were stream/river channel (KHP: canal bank; TBJ: near Tounsa Headwork's; ADS: near Treemu Headwork's), mountainous range (PCK: near mountain spring; PDK: muddy dunes along roadside; NSR: sandy-stone hills), hyper-arid area (DIS: Thal Desert; AHP: Cholistan Desert; DGK: flat plain with sandy dunes) and salt affected land (LSH: saline wasteland; KBL: hyper-saline lake; KKL: near salt lake).

2.4 Soil physical-chemical parameters

The soil taken from the root zone of each population in each habitat was utilized for physical-chemical characteristics. Sampling was done at two depth levels, i.e., 30 and 60 cm. Soil pH and electrical conductivity (EC) were assessed by making saturation paste of each soil sample by using a combined pH and EC meter (Cond 720, WTW series; Inolab, Weilheim, Germany), respectively. Soil ionic contents, i.e., Na^+, K^+, and Ca^{2+} were analyzed with the help of flame photometer (Jenway PFP-7, ELE Instrument Co. Ltd., Felsted, UK), while Cl^- content was estimated by digital chloride meter (Model 926, Sherwood Scientific Ltd., Cambridge, UK). Coordinates and elevation of each collection site were determined by using Google Earth Pro Software.

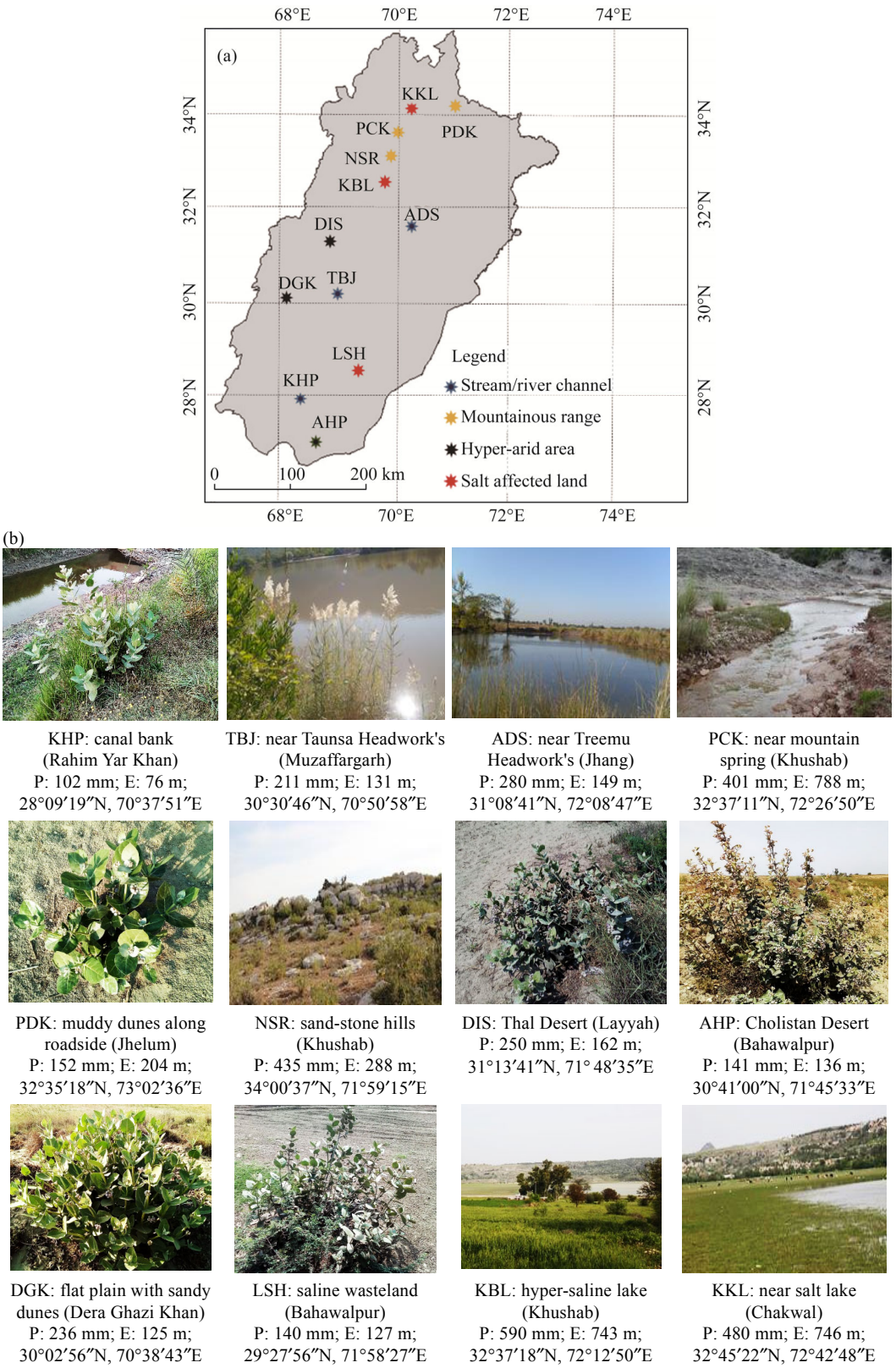

Fig. 1 Map showing collection sites (a) of *Calotropis procera* populations and its habitat characteristics (b) in the Punjab Province, Pakistan. P, precipitation, E, elevation. The abbreviations of these populations are the same in the following figures and tables.

2.5 Morphological parameters

Three average sized primary shoots were clipped from the base of each plant, and average was used for recording morphological characteristics. Morphological parameters including plant height, shoot (branch) length, shoot fresh, dry weight, leaf number, and leaf area were recorded. Clinometer was used for plant height, while measuring tape was used for shoot length measurements. Shoot fresh weight (SFW) was assessed immediately after their detachment and then dried in oven at 65°C until constant weight to assess shoot dry weight (SDW). Finally reading was taken by using digital loading balance. Leaf area was measured by using the following formula:

$$\mathrm{LA}=L\times W\times \mathrm{CF}, \tag{1}$$

where LA is the leaf area (cm^2); L is the length (cm); W is the width (cm); and CF is the correction factor (0.75).

2.6 Physiological parameters

2.6.1 Ionic contents

Plant samples were oven-dried at 65°C for analysis of inorganic ions. The ground dried samples were analyzed for Na^+, K^+, and Ca^{2+} after H_2SO_4 digestion (Wolf, 1982) using a flame photometer (Model 410, Sherwood Scientific Ltd., Cambridge, UK).

2.6.2 Photosynthetic pigments

Photosynthetic pigments (chlorophyll *a* (chl*a*), chlorophyll *b* (chl*b*), total chlorophyll (total chl), and carotenoids) were assayed by using the method of Arnon (1949). Fresh leaf material (0.1 g) was ground in 5 mL acetone (80%) and centrifuged at 14,000 r/m for 15 min at 4°C. The absorbance of the filtrate was recorded at 480, 645, and 663 nm by using spectrophotometer (IRMECO U2020, IRMECO GmbH & Co. KG, Lütjensee, Germany). Following formulas were used to calculate the final value:

$$\text{Chl } a=\left[12.7\left(\mathrm{OD663}\right)-2.69\left(\mathrm{OD645}\right)\right]\times\frac{V}{1000}\times W], \tag{2}$$

$$\text{Chl } b=\left[22.9\left(\mathrm{OD645}\right)-4.68\left(\mathrm{OD663}\right)\right]\times\frac{V}{1000}\times W], \tag{3}$$

$$\text{Total chl}=\left[20.2\left(\mathrm{OD645}\right)-8.02\left(\mathrm{OD663}\right)\right]\times\frac{V}{1000}\times W], \tag{4}$$

$$\text{Carotenoids}=\left[12.7\left(\mathrm{OD480}\right)-0.114\left(\mathrm{OD663}\right)\right]-0.638\left(\mathrm{OD645}\right)]/2500, \tag{5}$$

where OD is the optical density; V is the total volume of acetone extract (mL); and W is the fresh weight of the sample (g).

2.7 Biochemical parameters

2.7.1 Total soluble proteins (TSP)

To analyze TSP of samples, we followed the protocol of Bradford (1976). About 5 mL potassium phosphate buffer (pH 7.8) was used to prepare the homogenize mixture for each leaf sample. And 0.25 g leaf sample was crushed and ground in an ice chilled pestle and mortar until the extract was obtained. The extract was centrifuged in ultracentrifuge machine after maintaining the internal temperature constant (4°C) at 12,000 r/m. Totally 5 mL Bradford reagent and 100 μL extract were thoroughly mixed and vortexed for 10 s. The absorbance of each sample was measured through UV-spectrophotometer (IRMECO U2020, Lütjensee, Germany) at 595 nm wavelength.

2.7.2 Proline content

Fresh leaf sample was homogenized in 3% sulfo-salicylic acid for estimation of free proline content by following Bates et al. (1973) method. The extract was subjected to incubation with

acid ninhydrin and glacial acetic acid at 100°C, and finally extracted by dissolving toluene. The absorbance of each sample containing chromophore along toluene was observed on UV-spectrophometer (IRMECO U2020, Lütjensee, Germany) at 520 nm wavelength. Finally, standard curve was established to compute the final value of free proline content on a fresh weight basis.

2.7.3 Glycine betaine (GB)

Fresh leaf sample (0.25 g) was ground in 5 mL distilled water. The extract obtained was centrifuged on ultracentrifugation machine at 12,000 r/m for 15 min. About 500 µL mixture containing 1 mL sample and 1 mL 2 N H_2SO_4 was added in test tube and kept into refrigerator for 90 min. Moreover, 200.0 µL potassium triiodide, 2.8 mL distilled H_2O and 6.0 mL 1, 2-dichloroethane were added (Grieve and Grattan, 1983). Finally, absorbance was recorded at 365 nm wavelength by using UV-spectrophotometer (IRMECO U2020, Lütjensee, Germany).

2.7.4 Enzymatic antioxidants activities

Fresh leaf sample (0.25 g) was ground by using potassium phosphate buffer of pH 7.8 (5 mL) in ice chilled pestle and mortar. The extract was subjected to ultracentrifugation machine for 15 min at 12,000 r/m for precipitate separation. Finally, material was preserved in scientific refrigerator at –20°C for further analysis of enzyme activity, i.e., superoxide dismutase (SOD), catalase (CAT), and peroxidase (POD).

2.7.5 SOD

We determined SOD activity based on the principle of NBT (nitro blue tetrazolium) by following the method of Giannopolitis and Ries (1977). A homogenized mixture was prepared by mixing up of 50.0 µL sample extract, 0.1 mL L-methionine, 0.1 mL triton-X, 400.0 µL distilled water, 50.0 µL riboflavin, 50.0 µL NBT, and 1.0 mL potassium phosphate buffer (pH 7.0) under light for 20 min. The absorbance was recorded by using UV-spectrophotometer (IRMECO U2020, Lütjensee, Germany) at 560 nm wavelength.

2.7.6 CAT

Homogenized mixture (3.0 mL) containing potassium phosphate buffer (1.9 mL), along with H_2O_2 (1.0 mL), and sample extract (0.1 mL), was prepared to determine the activity of CAT enzyme by following Chance and Maehly (1955) method. Readings were taken using UV-spectrophotometer (IRMECO U2020, Lütjensee, Germany) at 240 nm wavelength.

2.7.7 POD

Chance and Maehly (1955) method was applied to measure POD activity. For analysis of each sample, 1.00 mL reaction mixture containing H_2O_2 (0.10 mL), leaf extract (0.05 mL), guaiacol solution (0.10 mL), and phosphate buffer (0.75 mL) was prepared. Finally, absorbance of each liquate was taken using UV-spectrophotometer (IRMECO U2020, Lütjensee, Germany) at 470 nm wavelength.

2.8 Anatomical parameters

For anatomical studies, the collected samples from each habitat were immediately kept in leak-proof plastic vials containing formalin acetic-alcohol solution (v/v formalin 5%, acetic acid 10%, ethanol 50%, and distilled water 35%), and subsequently put into acetic alcohol solution (v/v ethanol 75% and acetic acid 25%) after 2–3 d for longer period of preservation. A piece (1.5 cm) of topmost internode of main branch was taken for stem anatomy and 1.5-cm piece of mature leaf separated from leaf-center including midrib for leaf anatomy. Free-hand sectioning technique was applied for permanent slides preparation. Several grades of ethanol solutions (30%, 50%, 70%, 90%, and 100%) and xylene (100%) were used for sample dehydration and microbial resistance, and a combination of safranin (1%) and fast green (1%) for staining (Ruzin, 1999). Safranin stains secondary and lignified tissues (xylem vessels and sclerenchyma), while fast green stains primary tissues (parenchymatous tissue). After that sections were mounted under Canada

balsam. Micrographs of stained sections were taken on a digital camera (Nikon FDX-35, Tokyo, Japan) equipped with a stereo-microscope (Nikon 104, Tokyo, Japan). All parameters were measured through ocular micrometer calibrated with stage micrometer.

2.9 Statistical analysis

One-way ANOVA (analysis of variance) under CRD (complete randomized design) was applied on dataset for statistical analysis (Steel et al., 1997). The means were compared using LSD (least significance difference) by following Snedecor and Cochran (1980). PCA (principle component analysis) was used to check the influence of environmental factors on population's growth, physiology, and structural responses under various habitats. The statistical program R software v.4.0.1 was used to draw correlation matrix and density heatmap among various studied variables (species and environment) for estimation of correlation (R Development Core Team, 2017).

3 Results

3.1 Morphological characteristics

All populations of *C. procera* responded very differently for growth attributes relevant to habitat types (Table 2). Plant height was higher (4.1 m) in population AHP, which was followed (3.5 m) by DIS population. The minimum height (1.0 m) was recorded in PDK population. Shoot length was the maximum in AHP population (200.4 cm), followed by DIS population (173.8 cm). It was the minimum (65.2 cm) in KBL population. KHP population possessed the largest leaves (213.2 cm^2), followed by that in ADS population (180.0 cm^2). LSH population had the smallest leaves (46.8 cm^2).

The population DIS showed the highest number of leaves (172.4), followed by the leaf number (155.4) recorded in ADS population. PCK population represent the smaller number of leaves (49.2). The maximum shoot fresh weight (664.8 g/plant) was recorded in ADS population, which was significantly different (633.2 g/plant) from DIS population. The minimum (410.8 g/plant) of this attribute was observed in KHP population. Shoot dry weight was the maximum (277.2 g/plant) in TBJ population, followed by that in KBL population (260.4 g/plant). It was the minimum (84.4 g/plant) in NSR population.

3.1.1 Shoot ionic content

Variations regarding plant ionic contents were huge among populations (Table 2). The maximum value (67.6 mg/g d.wt.) of shoot Na^+ was observed in LSH population, followed by KBL population (63.4 mg/g d.wt.). Their minimum value (15.4 mg/g d.wt.) was seen in AHP and KHP populations. The maximum value (41.1 mg/g d.wt.) of shoot K^+ was noted in NSR population, followed by KKL population (32.7 mg/g d.wt.). Its minimum value (14.2 mg/g d.wt.) was recorded in DGK population. Shoot Ca^{2+} was the maximum (28.2 mg/g d. wt.) in NSR population, followed by PDK population. It was the minimum (13.8 mg/g d.wt.) in DGK population.

3.1.2 Photosynthetic pigments

Chlorophyll *a* content was the maximum (1.85 mg/g f.wt.) in AHP population, followed (1.72 mg/g f.wt.) by DGK population (Table 2). This parameter was the minimum (0.34 mg/g f.wt.) in LSH, KBL, and KKL populations. The maximum value (1.12 mg/g f.wt.) of chlorophyll *b* was recorded in AHP population, which was followed by that in ADS population (1.02 mg/g f.wt.). The minimum value (0.16 mg/g f.wt.) of this parameter was seen in three populations of LSH, KBL, and KKL. The population DGK showed the highest value (0.12 mg/g f.wt.) of carotenoids contents, this was followed (0.08 mg/g f.wt.) by AHP population. Their minimum value (0.01 mg/g f.wt.) was noted in KKL population. Total chlorophyll content was the highest (2.97 mg/g f.wt.) in AHP population, followed by DGK population. The lowest value (0.50 mg/g f.wt.) was recorded in populations of LSH, KBL, and KKL. The chlorophyll *a*/*b* ratio was the maximum (3.37) in KHP population, followed by TBJ population. The minimum value (1.13) of this parameter was found in ADS population. The maximum value (88.0) of Chl/Caro ratio was

Table 2 Morphological and physio-biochemical traits of *Calotropis procera* populations growing in different habitats of the Punjab Province, Pakistan

Index	Stream/river channel			Mountainous range			Hyper-arid area			Salt affected land			LSD	*F* value
	KHP	TBJ	ADS	PCK	PDK	NSR	DIS	AHP	DGK	LSH	KBL	KKL		
Morphological trait														
Plant height (m)	3.0^{c}	2.5^{d}	1.5^{f}	2.0^{e}	1.0^{i}	2.0^{e}	3.5^{b}	4.1^{a}	2.4^{d}	2.0^{e}	1.5^{f}	1.5^{f}	0.5	11.9***
Shoot length (cm)	86.4^{f}	94.4^{ef}	115.2^{d}	138.2^{cd}	150.4^{c}	86.4^{f}	173.8^{b}	200.4^{a}	100.2^{e}	100.2^{e}	65.2^{g}	115.8^{d}	15.3	4.8*
Leaf area (cm^2)	213.2^{a}	121.6^{d}	180.0^{b}	127.2^{cd}	82.0^{ef}	112.0^{de}	129.2^{cd}	148.8^{c}	85.2^{ef}	46.8^{f}	99.6^{e}	146.8^{c}	25.6	11.8***
Number of leaves per shoot	108.8^{d}	85.2^{e}	155.4^{b}	49.2^{g}	129.6^{c}	73.2^{ef}	172.4^{a}	57.2^{f}	62.4^{f}	102.4^{d}	85.2^{e}	124.8^{c}	16.1	10.5***
Shoot fresh weight (g/plant)	410.8^{i}	613.2^{c}	664.8^{a}	581.6^{d}	506.4^{g}	506.4^{g}	633.2^{b}	581.6^{d}	448.4^{h}	530.2^{f}	448.4^{h}	550.4^{e}	20.5	38.9***
Shoot dry weight (g/plant)	181.2^{k}	277.2^{a}	182.4^{d}	130.4^{f}	163.2^{e}	84.4^{i}	104.8^{h}	130.4^{f}	117.2^{g}	233.2^{c}	260.4^{b}	163.2^{e}	12.5	8.0**
Plant ionic content														
Shoot Na^+ (mg/g d.wt.)	15.4^{f}	29.0^{de}	33.4^{d}	32.2^{d}	30.8^{d}	27.9^{de}	25.6^{e}	15.4^{f}	22.7^{e}	67.6^{a}	63.4^{ab}	43.5^{c}	7.5	20.9***
Shoot K^+ (mg/g d.wt.)	20.4^{d}	19.8^{e}	22.0^{d}	28.3^{b}c	26.9^{c}	41.1^{a}	23.9^{cd}	19.1^{e}	14.2^{f}	28.0^{bc}	26.4^{c}	32.7^{b}	5.3	14.3***
Shoot Ca^{2+} (mg/g d.wt.)	18.9^{cd}	18.2^{cd}	24.5^{b}	18.4^{cd}	26.7^{ab}	28.2^{a}	16.9^{e}	24.2^{b}	13.8^{f}	16.8^{e}	21.1^{c}	20.1^{c}	3.4	22.2***
Photosynthetic pigment														
Chlorophyll *a* (mg/g f.wt.)	0.91^{h}	1.22^{f}	1.16^{g}	1.51^{d}	1.37^{e}	1.66^{c}	0.45^{i}	1.85^{a}	1.72^{b}	0.34^{j}	0.34^{i}	0.34^{i}	0.30	43.8***
Chlorophyll *b* (mg/g f.wt.)	0.27^{f}	0.54^{e}	1.02^{b}	0.77^{d}	0.72^{d}	0.76^{d}	0.22^{g}	1.12^{a}	0.86^{c}	0.16^{g}	0.16^{g}	0.16^{g}	0.50	26.6***
Carotenoids (mg/g f.wt.)	0.04	0.02^{ef}	0.04^{d}	0.05^{cd}	0.04^{d}	0.04^{d}	0.03^{de}	0.08^{b}	0.12^{a}	0.06^{c}	0.03^{de}	0.01^{f}	0.02	56.2***
Total chlorophyll (mg/g f.wt.)	1.18^{h}	1.76^{g}	2.18^{e}	2.28^{c}	2.09^{f}	2.32^{d}	0.67^{i}	2.97^{a}	2.58^{b}	0.50^{j}	0.50^{j}	0.50^{j}	0.40	30.3***
Chlorophyll a/b ratio	3.37^{a}	2.25^{b}	1.13^{g}	1.96^{e}	1.90^{e}	2.18^{c}	2.04^{d}	1.65^{f}	2.01^{d}	2.12^{c}	2.12^{c}	1.70^{e}	0.20	9.5**
Chl/Caro ratio	29.5^{f}	88.0^{a}	54.5^{c}	45.6^{d}	52.5^{c}	58.0^{b}	22.3^{g}	37.1^{e}	21.5^{h}	8.3^{j}	16.6^{i}	54.0^{c}	5.0	17.9***
Organic osmolyte														
Proline (μmol/g f.wt.)	24.9^{d}	22.5^{de}	13.1^{f}	22.3^{de}	13.1^{f}	19.7^{e}	22.8^{de}	25.9^{d}	14.4	43.3^{a}	34.0^{b}	29.5^{c}	4.5	23.1***
Glycine betaine (μmol/g f.wt.)	2.5^{bc}	2.9^{bc}	1.4^{cd}	3.7^{b}	3.1^{b}	2.0^{c}	1.0^{d}	2.3^{c}	1.9^{cd}	4.9^{ab}	5 .6^{a}	4.9^{ab}	1.5	9.6***
Total soluble protein (μg/g f.wt.)	204.0^{g}	333.7^{de}	91.6^{i}	208.2^{g}	358.4^{c}	102.1	320.8^{e}	222.8^{fg}	247.4^{f}	127.0^{h}	389.1^{b}	475.6^{a}	30.8	43.6***
Antioxidant														
SOD (U/μg protein)	1.0^{d}	1.4^{c}	1.7^{b}	1.3^{c}	0.9^{de}	0.7^{e}	1.6^{b}	1.1^{d}	2.0^{a}	2.0^{a}	1.6^{b}	1.5^{bc}	0.3	27.5***
CAT (U/μg protein)	1.1^{e}	1.2^{e}	0.8^{g}	0.5^{h}	1.6^{c}	0.9^{fg}	1.4^{d}	1.0^{f}	1.3^{d}	1.8^{b}	2.0^{a}	1.8^{b}	0.2	44.8***
POD (U/μg protein)	1.7^{c}	1.1^{e}	1.4^{d}	1.0^{ef}	0.7^{f}	1.0^{ef}	-	1.3^{de}	1.7^{c}	2.1^{a}	1.9^{b}	1.6^{cd}	0.2	20.1***

Note: Different lowercase letters within each row indicate significant difference among different populations at $P<0.05$ level. *, **, and *** indicate the significances at $P<0.05$, $P<0.01$, and $P<0.001$ levels, respectively. LSD, least significance difference. SOD, superoxide dismutase; CAT, catalase; POD; peroxidase; d.wt., dry weight; f.wt., fresh weight; - means no value.

recorded in TBJ population, followed by NSR population. Their minimum value (8.3) was noted in LSH population.

3.1.3 Organic osmolyte

Proline content was the highest (43.3 μmol/g) in LSH population, followed by KBL population (Table 2). The minimum value (13.1 μmol/g) was recorded in populations of PDK and ADS. The maximum (5.6 μmol/g f.wt.) of GB content was found in KBL population, followed by LSH and KKL populations. The minimum value (1.0 μmol/g f.wt.) was found in DIS population. Population KKL showed the maximum value (475.6 μg/g f.wt.) of total soluble proteins, followed by KBL population. The minimum value (91.6 μg/g f.wt.) was observed in ADS population.

3.1.4 Antioxidant

The maximum value (2.0 U/μg protein) of SOD was recorded in populations of DGK and LSH, which was not significantly varied (1.7 U/μg protein) from ADS population. Their minimum value (0.7 U/μg protein) was noted in NSR population. KBL population possessed the highest value (2.0 U/μg protein) of CAT, which was close (1.8 U/μg protein) to populations KKL and LSH. The minimum value (0.5 U/μg protein) was found in PCK population. LSH population showed the maximum (2.1 U/μg protein) of POD (peroxidase), followed by KBL population. PDK population had a low amount (0.7 U/μg protein) of POD (Table 2).

3.2 Anatomical characteristics

3.2.1 Stem anatomy

Huge variations regarding stem anatomical attributes were seen in differently adapted populations of *C. procera* (Table 3; Fig. 2). They showed remarkable modifications in size, nature and shape of dermal, vascular, and storage tissues. DIS population showed widened stem radius (1988.3 μm), followed by DGK population. The narrowest stem radius (1506.7 μm) was found in KBL population. Thick cuticle (51.5 μm) was seen in AHP population, followed by NSR population. Thin cuticle (18.4 μm) was observed in two populations of ADS and KBL. NSR population showed the largest epidermal cell area (663.5 μm^2), followed by DIS and KBL populations. PCK population indicated the smallest epidermal cell area (231.3 μm^2) than the rest of populations.

Thick collenchyma layer (100.7 μm) was recorded in PCK population, followed by DGK, LSH, and KKL populations. Thin collenchyma layer (48.8 μm) was found in populations of AHP, NSR, and KHP. Enlarged cortical region (198.9 μm) was noted in AHP population, followed by DGK, TBJ, and KHP populations. This was greatly reduced (58.9 μm) in NSR population. The largest cortical cell area (252.2 μm^2) was recorded in AHP population, followed by KHP population. Their smaller cell area (35.2 μm^2) was noted in two populations of ADS and PCK. Intensive sclerification (790.4 μm) was seen in populations of PDK and KBL, followed by TBJ population. The minimum (263.3 μm) was found in DGK population.

DIS population possessed widened metaxylem area (247.0 μm^2), followed by LSH population. The narrowest xylem area (23.5 μm^2) was found in KBL population. Two populations of AHP and LSH showed the largest outer phloem region (588.9 μm^2), followed by PCK population. The smallest region (58.3 μm^2) was noted in KHP population. KKL population showed the broadest inner phloem region (503.0 μm^2), its closed value was found in LSH population. The narrowest phloem region (85.2 μm^2) was noted in NSR and KHP populations. DIS population had enlarged pith thickness (352.1 μm), followed by LSH and ADS populations. The reduced pith thickness (111.3 μm) was found in KBL and TBJ populations. The largest pith cell area (217.2 μm^2) was found in two LSH and AHP populations, followed by KKL population. The smallest pith cell area (41.4 μm^2) was recorded in TBJ population (Table 3; Fig. 2).

Table 3 Stem anatomical traits of *Calotropis procera* populations growing in different habitats of the Punjab Province, Pakistan

Index	Stream/river channel			Mountainous range			Hyper-arid area			Salt affected land			LSD	*F* value
	KHP	TBJ	ADS	PCK	PDK	NSR	DIS	AHP	DGK	LSH	KBL	KKL		
Stem radius (μm)	1696.7^{d}	1633.3^{e}	1918.3^{b}	1696.7^{d}	1696.7^{d}	1955.8^{ab}	1988.3^{a}	1860.0^{c}	1918.3^{b}	1855.0^{c}	1506.7^{f}	1849.2^{c}	59.5	2.4^{NS}
Cuticle thickness (μm)	36.4^{bc}	37.4^{bc}	18.4^{e}	31.4^{cd}	38.4^{bc}	40.4^{b}	31.4c^{d}	51.5^{a}	26.7^{d}	34.1^{c}	18.4^{e}	36.1b^{c}	7.4	8.4**
Epidermal cell area (μm^2)	425.9^{cd}	362.7^{de}	450.5^{c}	231.3^{e}	387.5^{d}	663.5^{a}	638.3^{ab}	380.0^{d}	567.3^{b}	348.8^{de}	638.3^{ab}	350.2^{de}	50.0	10.8**
Collenchyma thickness (μm)	48.8^{d}	55.8^{cd}	64.2^{c}	100.7^{a}	55.8^{cd}	48.8^{d}	60.9^{c}	48.8^{d}	75.9^{b}	75.9^{b}	62.6^{c}	75.9^{b}	10.5	8.4**
Cortical region thickness (μm)	168.3^{b}	168.3^{b}	83.5^{cd}	84.8^{cd}	96.2^{c}	58.9^{d}	79.3^{cd}	198.9^{a}	168.3^{b}	90.0^{c}	108.0^{c}	106.0^{c}	32.7	15.1***
Cortical cell area (μm^2)	212.0^{b}	90.1^{e}	35.2^{f}	35.2^{f}	105.5^{d}	153.2^{c}	78.6^{e}	252.2^{a}	142.1^{c}	78.5^{e}	99.5^{d}	143.9^{c}	33.3	28.2***
Sclerenchyma thickness (μm)	564.2^{d}	775.0^{ab}	664.6^{c}	693.3^{b}	790.4^{a}	700.4^{b}	300.0^{g}	400.0^{f}	263.3^{h}	303.0^{g}	790.4^{a}	511.0^{e}	28.9	1.1^{NS}
Metaxylem area (μm^2)	41.8^{ef}	105.5^{c}	102.1^{c}	99.0^{c}	73.6^{d}	96.7^{c}	247.0^{a}	50.0^{e}	71.7^{d}	201.2^{b}	23.5^{f}	118.8^{c}	34.1	28.3***
Outer phloem area (μm^2)	58.3^{e}	166.7^{d}	244.2^{c}	453.6^{b}	105.5^{d}	136.7^{d}	229.4^{c}	588.9^{a}	180.6^{cd}	588.9^{a}	118.5^{d}	214.5^{c}	80.8	24.7***
Inner phloem area (μm^2)	85.2^{f}	193.2^{d}	204.2^{d}	326.2^{c}	156.7^{de}	85.2^{f}	160.0^{de}	312.9^{c}	203.3^{d}	431.1^{b}	116.6^{e}	503.0^{a}	89.1	20.2***
Pith thickness (μm)	216.1^{c}	111.3^{e}	298.9^{b}	183.3^{d}	249.8^{bc}	170.3^{d}	352.1^{a}	217.9^{c}	214.6^{c}	298.9^{b}	111.3^{e}	186.0^{d}	49.3	14.1***
Pith cell area (μm^2)	163.2^{c}	41.4^{g}	106.2^{e}	148.3^{c}	73.6^{f}	158.5^{c}	132.6^{d}	217.2^{a}	127.4^{d}	217.2^{a}	97.5^{e}	190.0^{b}	31.0	11.8**

Note: Different lowercase letters within each row indicate significant difference among different populations at P<0.05 level. ** and *** indicate the significances at P<0.01, and P<0.001 levels, respectively. ^{NS}, not significant; LSD, least significance difference.

3.2.2 Leaf anatomy

Various populations of *C. procera* showed very specific leaf anatomical modifications in response to varied environmental conditions (Table 4; Fig. 3). Two populations of DIS and KHP showed thick leaf midrib (5517.9 μm), followed by AHP population. The minimum value (1018.3 μm) was found in LSH population. AHP population showed very thick lamina (246.5 μm), its closed value was seen in DGK population. Thin lamina (83.2 μm) was noted in PCK population. DIS population possessed the largest epidermal cell area (101.0 μm^2), followed by LSH population. The smaller cell area (16.2 μm^2) was noted in populations of ADS and KHP. KBL and AHP populations had thick cuticle (35.3 μm), followed by KKL and PCK populations. Thin cuticle (13.0 μm) was noted in ADS population. Intensive sclerification (846.5 μm) was observed in KBL population, followed by TBJ population. The reduced tissue sclerification (147.8 μm) was noticed in ADS population. DIS population had the largest cortical thickness (1067.7 μm), followed by KHP population. The reduced proportion (262.8 μm) of cortex was found only in AHP population. Two populations of KKL and DIS showed the largest cells of cortex (432.0 μm^2), followed by KHP population. The smallest cells (146.6 μm^2) were recorded in LSH population.

DIS population showed widened xylem vessels (633.2 μm^2), followed by TBJ population. The narrowest xylem vessels (183.4 μm^2) were found in PDK population. The maximum phloem area (301.2 μm^2) was measured in two populations of TBJ and KKL, its closed value was

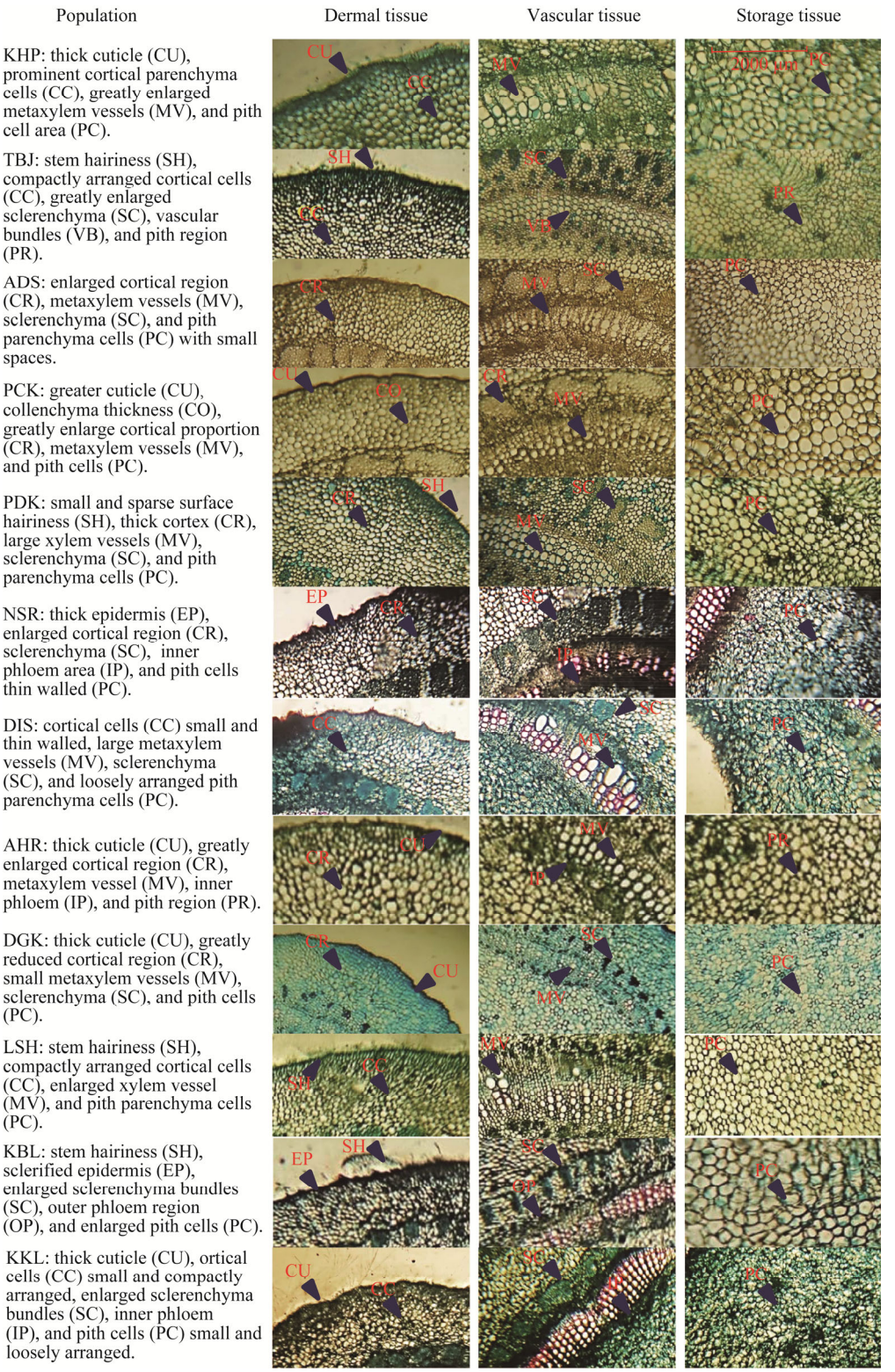

Fig. 2 Transverse sections showing different stems tissues of *Calotropis procera* populations collected from different habitats of the Punjab Province, Pakistan

recorded in AHP population. The minimum phloem area (101.9 μm^2) was observed in PCK and PDK populations. The largest trichome area (355.2 μm^2) was found in PCK population, followed

by AHP population. The smallest trichome area (61.9 μm^2) was found only in DGK population. AHP population showed very dense trichome on leaf surface (119.2/mm^2), followed by PCK population. The lowest density (40.5/mm^2) was noticed in two populations of DGK and KBL (Table 4; Fig. 3).

Table 4 Leaf anatomical traits of *Calotropis procera* populations growing in different habitats of the Punjab Province, Pakistan

Index	Stream/river channel			Mountainous range			Hyper-arid area			Salt affected land			LSD	*F* value
	KHP	TBJ	ADS	PCK	PDK	NSR	DIS	AHP	DGK	LSH	KBL	KKL		
Midrib thickness (μm)	5517.9^{a}	4273.7^{c}	2288.3^{g}	3365.6^{f}	4132.1^{d}	4135.4^{d}	5517.9^{a}	4398.3^{b}	1198.3^{h}	1018.3^{i}	3796.2^{e}	1195.0^{h}	500.9	272.3***
Lamina thickness (μm)	176.1^{e}	103.9^{g}	198.9^{c}	83.2^{h}	223.6^{bc}	176.4^{e}	183.3^{d}	246.5^{a}	232.1^{b}	194.7^{c}	132.0^{f}	133.8^{f}	11.2	80.4***
Epidermal cell area (μm^2)	16.2^{g}	39.3^{e}	16.2^{g}	20.1^{f}	85.0^{bc}	21.6^{f}	101.0^{a}	85.9b^{c}	74.3^{c}	89.3^{b}	46.0^{d}	84.3^{bc}	4.7	201.5***
Cuticle thickness (μm)	28.8^{c}	32.0^{b}	13.0^{f}	33.4^{ab}	19.3^{d}	16.0^{e}	18.7^{d}	35.3^{a}	28.0^{c}	18.8^{d}	35.3^{a}	33.4^{ab}	2.7	34.3***
Sclerenchyma thickness (μm)	723.0^{c}	771.3^{b}	147.8^{j}	155.4^{i}	296.8^{h}	504.3^{e}	501.5^{e}	154.5^{i}	448.1^{f}	313.0^{g}	846.5^{a}	548.4^{d}	39.4	104.2***
Cortical thickness (μm)	990.5^{b}	641.6^{d}	896.6^{c}	389.9^{g}	614.0^{de}	610.4^{de}	1067.7^{a}	262.8^{h}	672.4^{d}	853.0^{c}	567.8^{e}	470.4^{f}	75.8	42.3***
Cortical cell area (μm^2)	385.3^{b}	251.2^{e}	161.3^{h}	231.4^{f}	176.3^{g}	260.7^{e}	432.0^{a}	294.3^{d}	176.5^{g}	146.6^{i}	307.7^{c}	432.0^{a}	21.3	530.6***
Metaxylem area (μm^2)	530.1^{b}	608.5^{ab}	511.5^{bc}	423.4^{c}	183.4^{f}	266.1^{e}	633.2^{a}	583.6^{ab}	443.2^{c}	364.3^{d}	537.7^{b}	493.8^{bc}	76.1	19.0***
Phloem area (μm^2)	139.4^{g}	301.2^{a}	161.3^{f}	101.9^{i}	101.9^{i}	232.9^{d}	166.7^{f}	285.3^{b}	115.6^{h}	172.6^{e}	242.7^{c}	301.2^{a}	23.2	303.3***
Trichome area (μm^2)	137.8^{h}	261.4^{c}	207.3^{e}	355.2^{a}	108.1^{i}	144.4^{g}	81.2^{j}	280.1^{b}	61.9^{k}	258.1^{d}	174.9^{f}	81.7^{j}	19.8	929.3***
Trichome density (individuals/mm^2)	52.6^{f}	79.9^{d}	49.3^{g}	100.8^{b}	49.9^{g}	69.3^{e}	49.5^{g}	119.2^{a}	40.5^{h}	85.3^{c}	40.5^{h}	90.3^{c}	6.6	151.0***
Adaxial stomatal area (μm^2)	914.2^{b}	827.7^{d}	957.3^{a}	432.2^{j}	700.8^{g}	685.1^{h}	682.6^{h}	796.0^{e}	718.0^{f}	496.3^{i}	795.5^{e}	861.4^{c}	21.0	1657.5***
Abaxial stomatal area (μm^2)	842.9^{b}	524.4^{d}	737.0^{c}	100.3^{i}	83.8^{j}	100.2^{i}	269.0^{g}	881.4^{a}	83.8^{j}	121.5^{h}	508.6^{e}	404.9^{f}	20.5	3545.1***
Adaxial stomatal density (individuals/mm^2)	35.0^{d}	50.0^{a}	45.0^{b}	40.0^{c}	35.0^{d}	32.0^{de}	32.0^{de}	23.0^{f}	29.0^{e}	26.0^{ef}	31.0^{e}	28.0^{e}	5.8	100.2***
Abaxial stomatal density (individuals/mm^2)	27.0^{b}	26.0^{b}	29.0^{ab}	21.0^{c}	31.0^{a}	16.0^{d}	20.0^{c}	31.0^{a}	27.0^{b}	21.0^{c}	29.0^{ab}	29.0^{ab}	3.2	73.9***

Note: Different lowercase letters within each row indicate significant difference among different populations at P<0.05 level. *** indicate the significance at P<0.001 level. LSD, least significance difference.

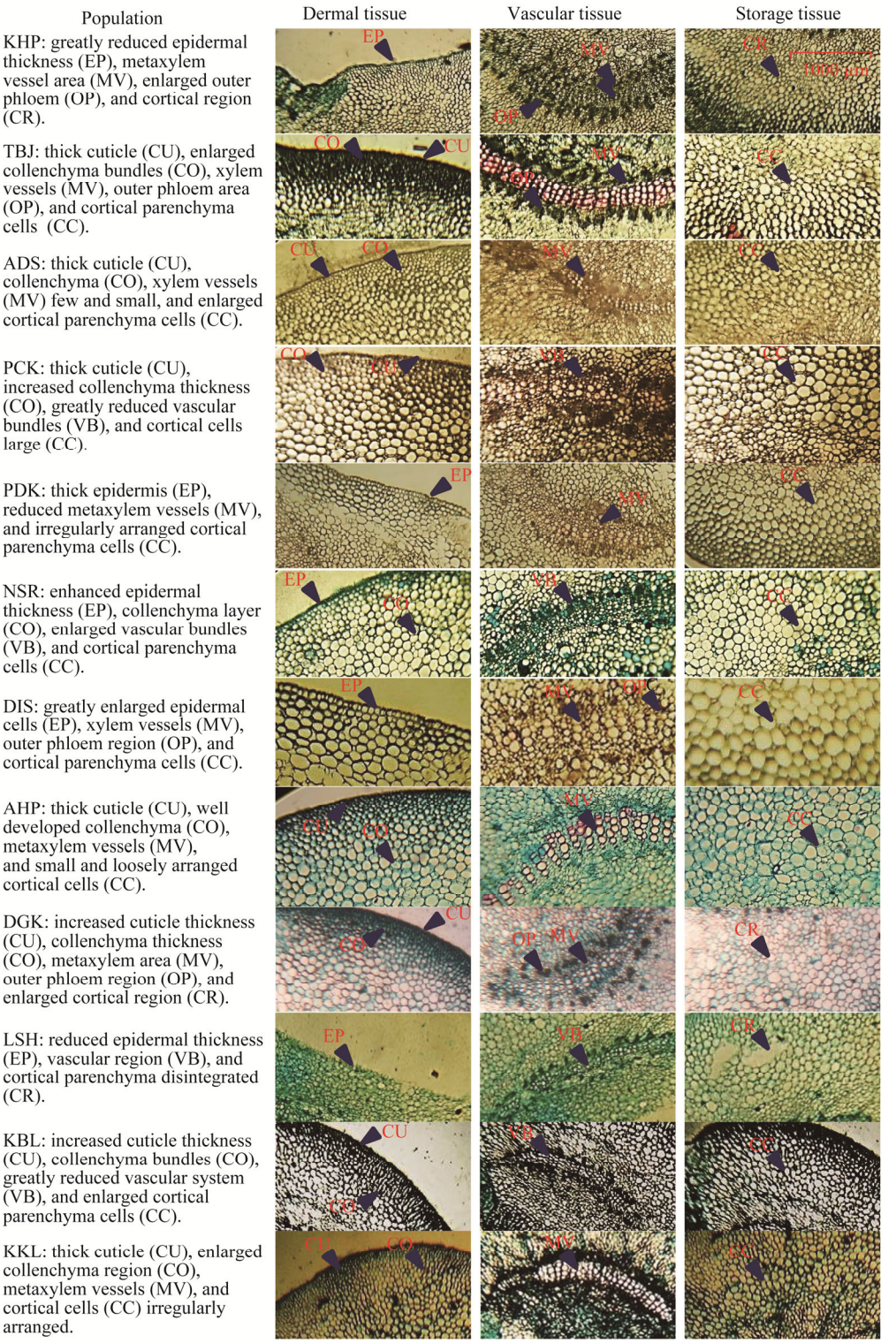

Fig. 3 Transverse sections showing different leaf tissues of *Calotropis procera* populations collected from different habitats of the Punjab Province, Pakistan

The maximum stomatal size (957.3 μm^2) on adaxial surface of leaf was noticed in ADS population, followed by KHP population. The minimum size of stomata (432.2 μm^2) was recorded in PCK population. On the other hand, the largest stomatal size (881.4 μm^2) on abaxial

surface was measured in AHP population, followed by KHP population. The smallest size of stomata (83.8 μm^2) was recorded in two populations of PDK and PCK. The adaxial stomatal density was the maximum (50.0/mm^2) in TBJ population, followed by ADS population. The minimum stomatal density (23.0/mm^2) was found only in AHP population. The maximum abaxial stomatal density (31.0/mm^2) was recorded in two populations of AHP and PDK. Its closed value was seemed in three populations of KBL, KKL, and ADS. The minimum of this attribute (16.0/mm^2) was observed in NSR population (Table 4; Fig. 4).

3.3 Multivariate analysis

PCA was applied on data to check the influence of environmental factors on growth, physiological, and anatomical attributes of different populations of *C. procera* (Fig. 5a–d).

3.3.1 Influence of soil physical-chemical attributes on growth and physiology

Plant height, leaf number, and shoot length were strongly influenced in AHP population, while leaf area was greatly influenced in KHP population rich in soil Ca^{2+}. Shoot dry weight was influenced by soil EC, Na^+, and Cl^- of LSH and KBL populations, whereas shoot fresh weight was greatly influenced by soil K^+ in DIS population. In case of plant physiology, SOD, shoot K^+, shoot Na^+, and proline showed strong impacts of soil Na^+ in KKL population, while GB, CAT, and POD represent the effects of soil EC and Cl^- in KBL population. Photosynthetic pigments like Chlorophyll *a*, Chlorophyll *b*, and total chlorophyll showed strong association with AHP population rich in soil K^+, but the carotenoids showed association with PCK population impregnated by soil Ca^{2+}.

3.3.2 Influence of soil physical-chemical attributes on anatomy

In case of stem attributes, sclerenchyma thickness showed positive relation with KBL population, while collenchyma thickness showed positive relation with LSH population under varying level of soil EC, Na^+, and Cl^-. Cuticle thickness and stem radius showed association with DGK population, whereas cortical cell area, cortical region thickness, and epidermal cell area showed associated with soil pH in DIS population. Among leaf anatomical attributes, cuticle thickness was strongly influenced in KKL population, while trichome area and trichome density were influenced by soil Ca^{2+} in PCK population. In NSR population, metaxylem area and lamina thickness were associated with soil K^+, adaxial stomatal area and abaxial stomatal area in TBJ population, while adaxial stomatal density and cortical region thickness showed close association with AHP population.

3.4 Correlation matrix and density heatmaps

The soil physical-chemical traits and morpho-physiological traits exhibited a significant (P<0.01) correlation (Fig. 6a). Soil physical-chemical traits, i.e., Cl^-, Na^+, and EC reflected a strong positive correlation with osmolytes like proline and GB, and with antioxidant enzymes (CAT and POD). Similarly, shoot Na^+ was positively correlated with organic osmolytes and cellular antioxidants. Soil and shoot K^+ and Ca^{2+} were negatively correlated with antioxidants. Clustered heatmap was constructed between soil physical-chemical traits and morpho-physiological traits to visualize the association between studied traits. Soil EC, Na^+, and Cl^- exhibited a strong relation with shoot Na^+, shoot dry weight, POD, and SOD, while a negative association was assessed between photosynthetic pigments and soil traits. Moreover, a distinct clustering was observed between soil traits and morpho-physiological characters (Fig. 6b).

The soil physical-chemical characters possessed a significant influence on stem structural attributes as presented in Figure 7a. The positive correlation was passed between Na^+ and inner phloem area, stem radius, pith thickness, inner phloem area, and pith cell area. However, a strong negative influence was observed of Ca^{2+} with epidermal cell area, pith cell area and sclerenchymatous thickness. Soil Cl^-, Na^+, and EC indicate a strong association with outer phloem area, inner phloem area, and cortical cell area. A negative association was observed

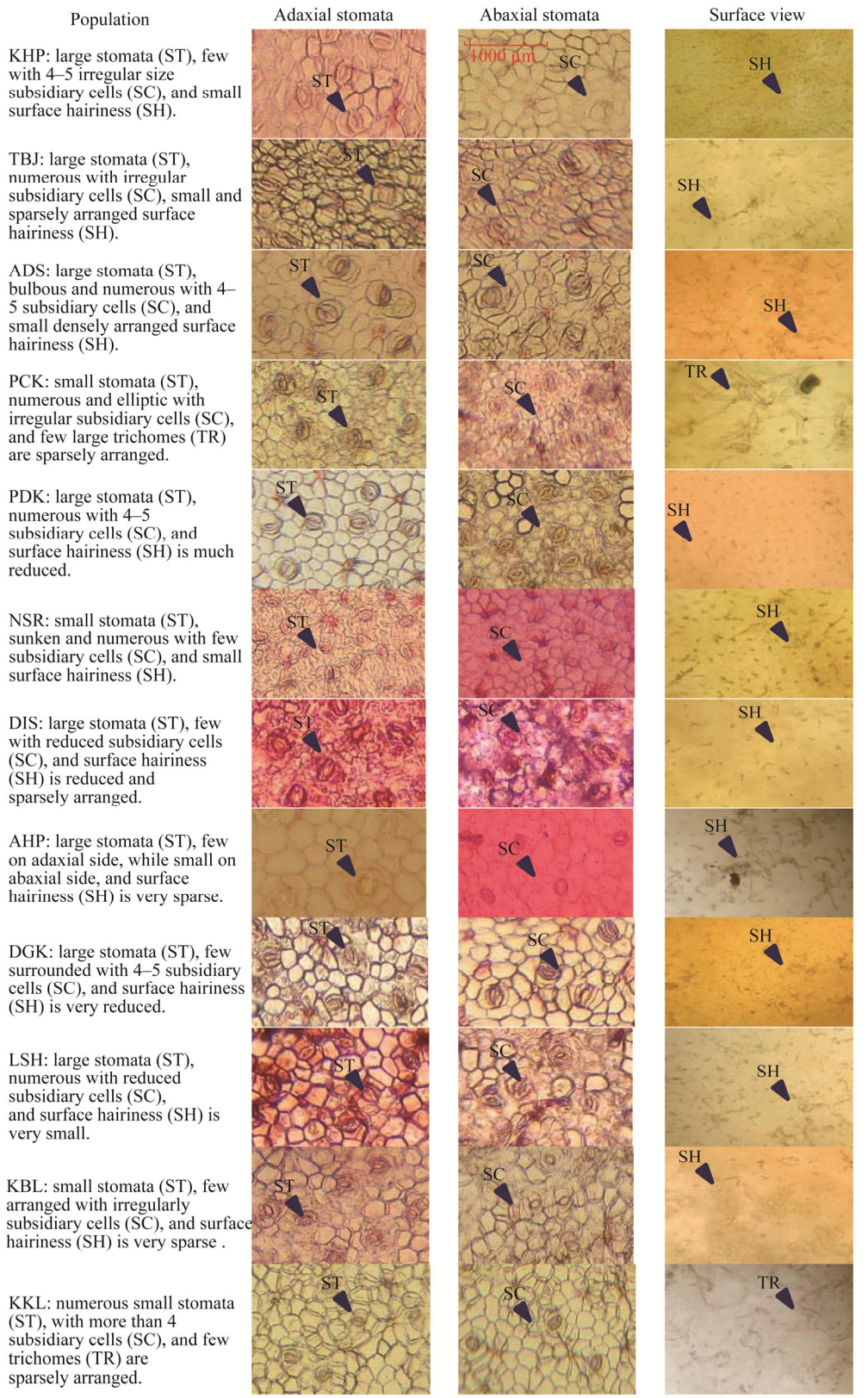

Fig. 4 Transverse sections showing epidermal surface view of *Calotropis procera* populations collected from different habitats of the Punjab Province, Pakistan

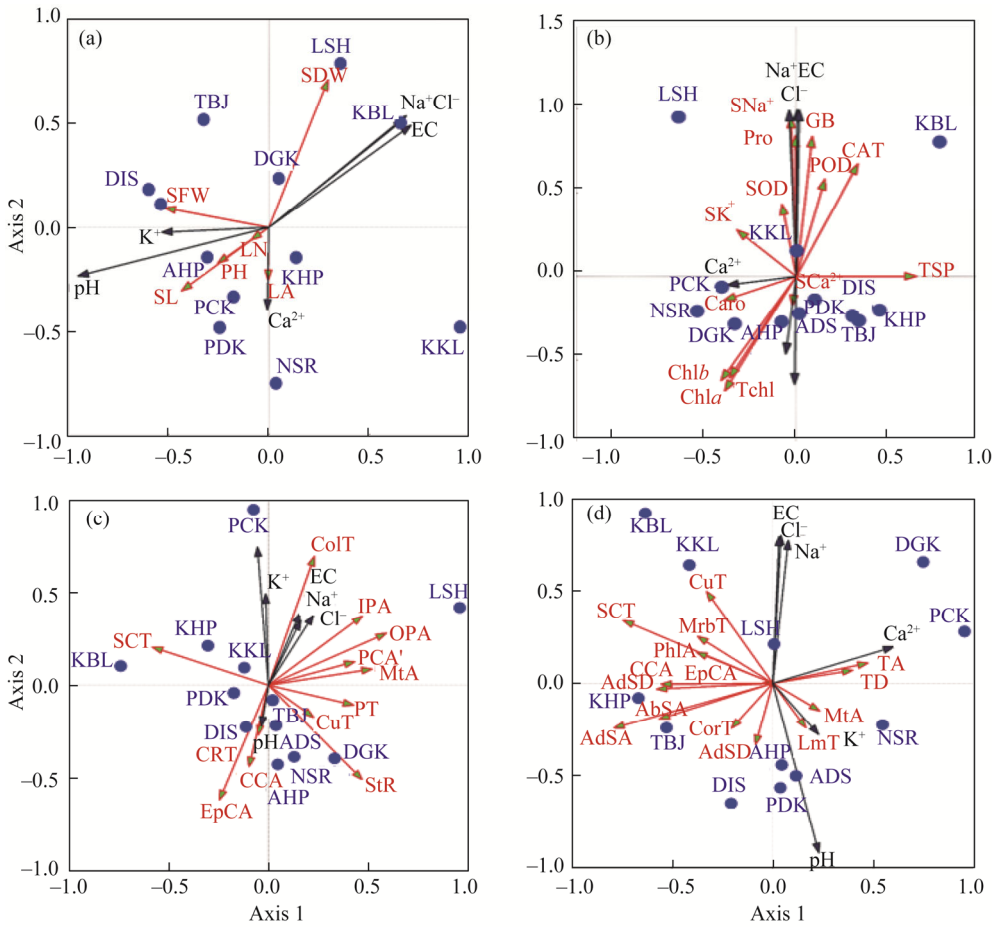

Fig. 5 PCA (principle component analysis) showing association of soil physical-chemical characteristics with growth (a), physiology (b), stem (c), and leaf anatomical attributes (d) of *Calotropis procera* populations collected from different habitats of the Punjab Province, Pakistan. PH, plant height; LN, number of leaves; LA, leaf area; SL, shoot length; SFW, shoot fresh weight; SDW, shoot dry weight; SNa^+, shoot Na^+; SK^+, shoot K^+; SCa^{2+}, shoot Ca^{2+}; Chl*a*, Chlorophyll *a*; Chl*b*, Chlorophyll *b*; Caro, carotenoids; Tchl, total chlorophyll; Pro, proline; GB, glycine betaine; TSP, total soluble proteins; SOD, superoxide dismutase; CAT, catalase; POD, peroxidase; Ca^{2+}, soil Ca^{2+}; K^+, soil K^+; Na^+, soil Na^+; Cl^-, soil Cl^-; EC, electrochemical conductivity; pH, soil pH; CuT, cuticle thickness; StR, stem radius; CCA, cortical cell area; EpCA, epidermal cell area; CRT, cortical thickness; SCT, sclerenchymatous thickness; ColT, collenchymatous thickness; IPA, inner phloem area; OPA, outer phloem area; PCA', epidermal cell area; MtA, metaxylem area; PhlA, phloem area; TA, trichome area; TD, trichome density; LmT, lamina thickness; AdSD, adaxial stomatal density; CorT, cortical region thickness; AdSA, adaxial stomatal area; AbSA, abaxial stomatal area; AbSD, abaxial stomatal density; MrbT, midrib thickness. The abbreviations are the same in figures 6, 7 and 8.

between epidermal cell area, cortical cell area, outer phloem area, inner phloem area, and stem radius with pith thickness (Fig. 7b). A correlation matrix between soil physical-chemical attributes and leaf structural traits indicated a significant (P<0.01) correlation. A strong positive correlation was assessed of trichome area and trichome density with Ca^{2+}. The phloem area, Ca^{2+}, Na^+, and adaxial stomatal density presented a significant negative correlation (Fig. 8a). Leaf anatomical traits exhibited a strong clustering with soil K^+ and Ca^{2+}, while sclerenchymatous thickness grouped with midrib thickness, epidermal cell area with lamina thickness, and abaxial stomatal area with adaxial stomatal area. Soil Cl^-, Na^+, and EC showed a strong influence on phloem area, cortical cell area, abaxial stomatal area, adaxial stomatal area, and abaxial stomatal density. Density pattern was varied among all studied traits (Fig. 8b).

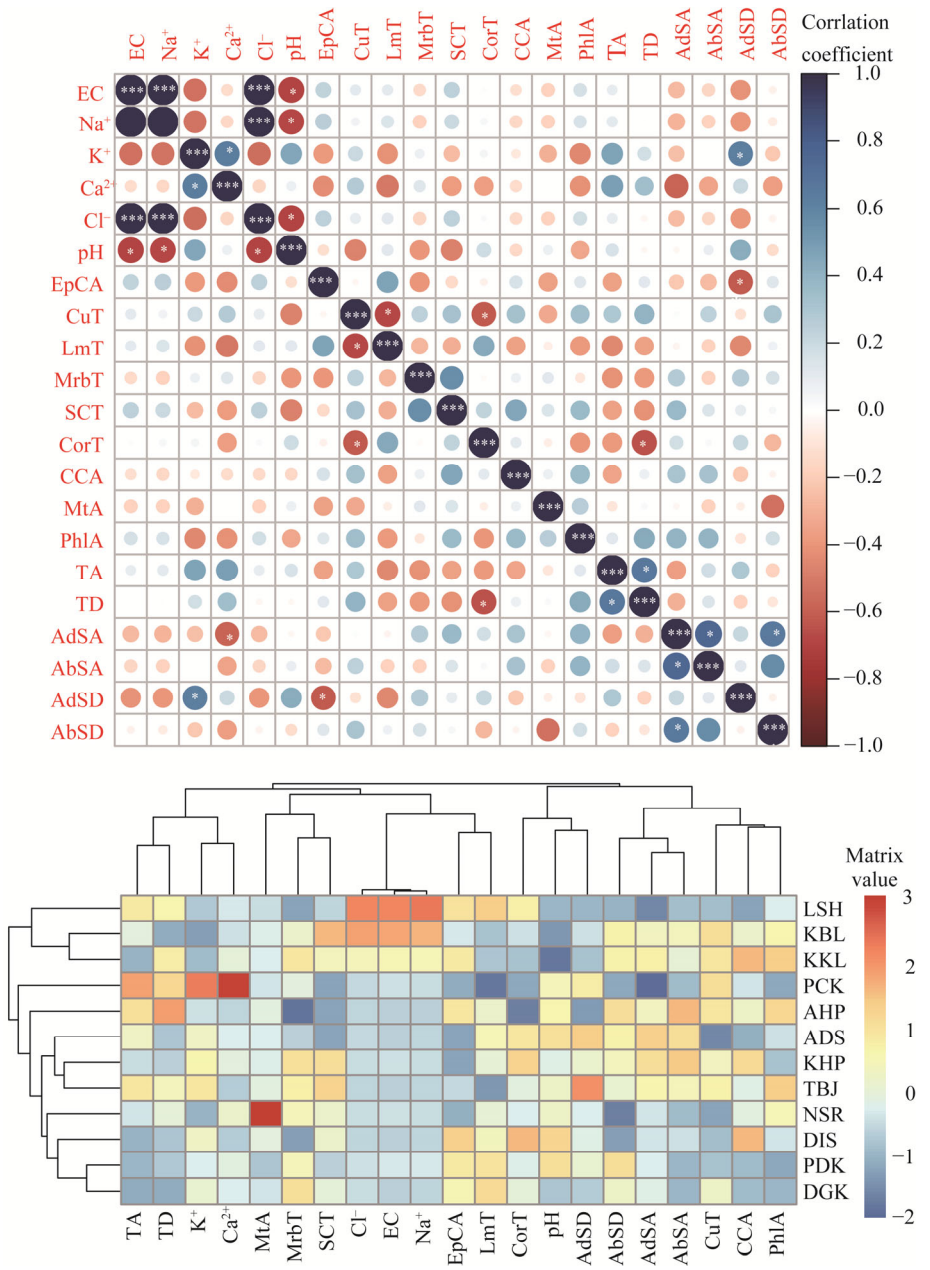

Fig. 6 (a), correlation among soil physical-chemical traits and morpho-physiological attributes, and (b), density heatmap for soil physical-chemical traits and morpho-physiological attributes of *Calotropis procera* populations collected from different habitats of the Punjab Province, Pakistan. *, $P<0.05$ level; ***, $P<0.01$ level.

4 Discussion

Huge variations regarding growth attributes were recorded among populations due to great environmental heterogeneity. These characteristics were genetically fixed over prolonged time of evolution in these populations, and these are representative of their respective habitats (Paccard et al., 2013). Growth attributes are considered as important criteria to estimate the response and tolerance potential of population to prevailing stressful condition (El-Hendawy et al., 2017). In this study, the individuals adapted to hyper-arid areas like AHP and DIS had the highest height and shoot size, compared with individuals of other habitats. It may be apparently due to

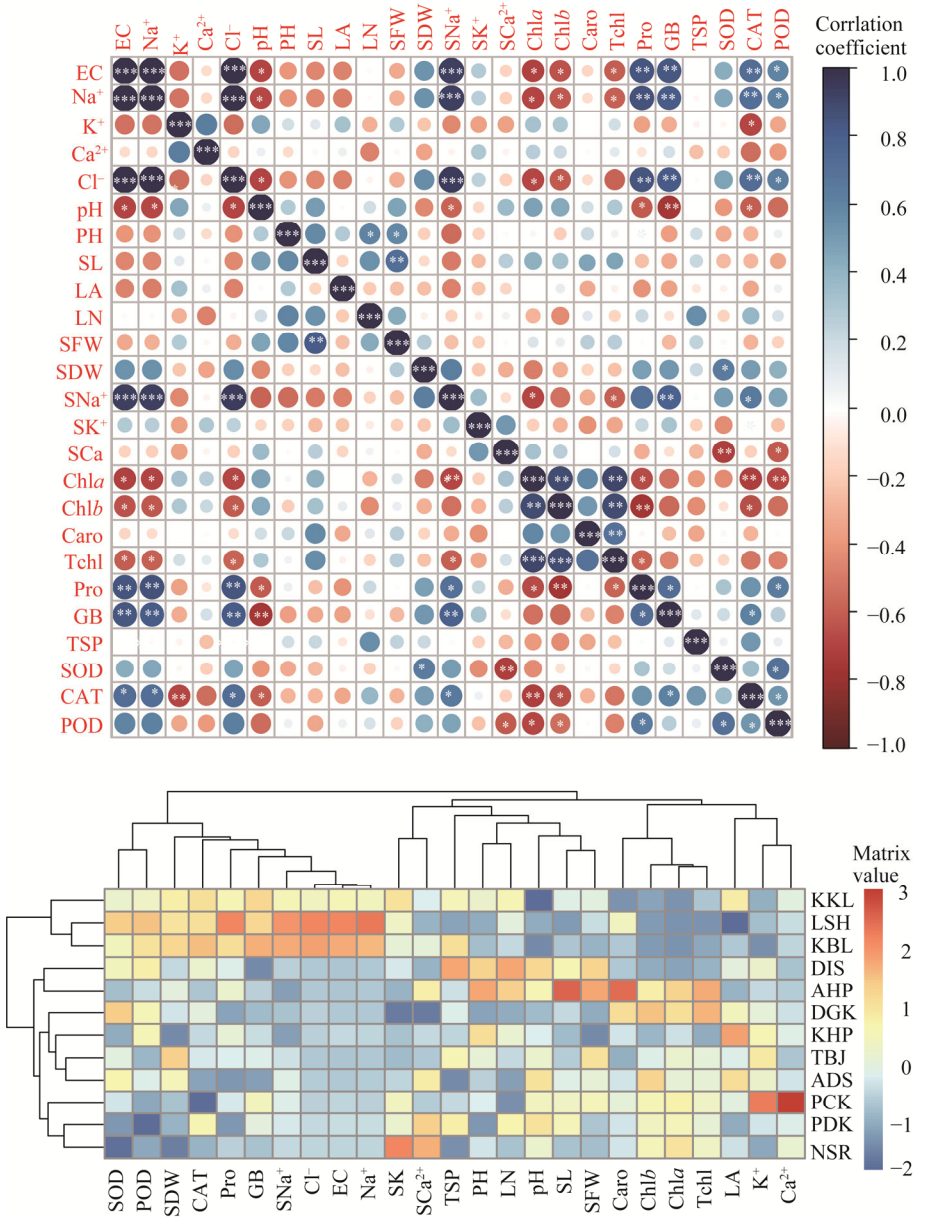

Fig. 7 (a), correlation among soil physical-chemical traits and stem structural attributes; (b), cluster heatmap for soil physical-chemical traits and stem structural attributes of *Calotropis procera* populations collected from different habitats of the Punjab Province, Pakistan. *, $P<0.05$ level; **, $P<0.01$ level; ***, $P<0.001$ level.

less anthropogenic activities (i.e., cultivation, cutting, and burning), reduced grazing impact, and episodic water resources like annual precipitation and flooded irrigation. In earlier reports, it was clearly mentioned that *Calotropis* is a drought resistance and salt-tolerant plant, and can grow in different ranges of soil type. The populations growing in salt affected lands showed much reduced growth attributes such as plant height, shoot growth, leaf number and size, and biomass production. It could be result of depressive effect of salinity on growth attributes. Many researchers have reported that it can tolerate salinity to some extent and cannot sustain under high soil salinity (Boutraa, 2010; Hassan et al., 2015).

Leaves are main photosynthetic organs of plants and thus exceptionally vital for growth and biomass accumulation (De Faria et al., 2018). Formation of large leaves in KHP is a principal strategy in order to prevent from seasonally occurring water shortage due to low precipitation

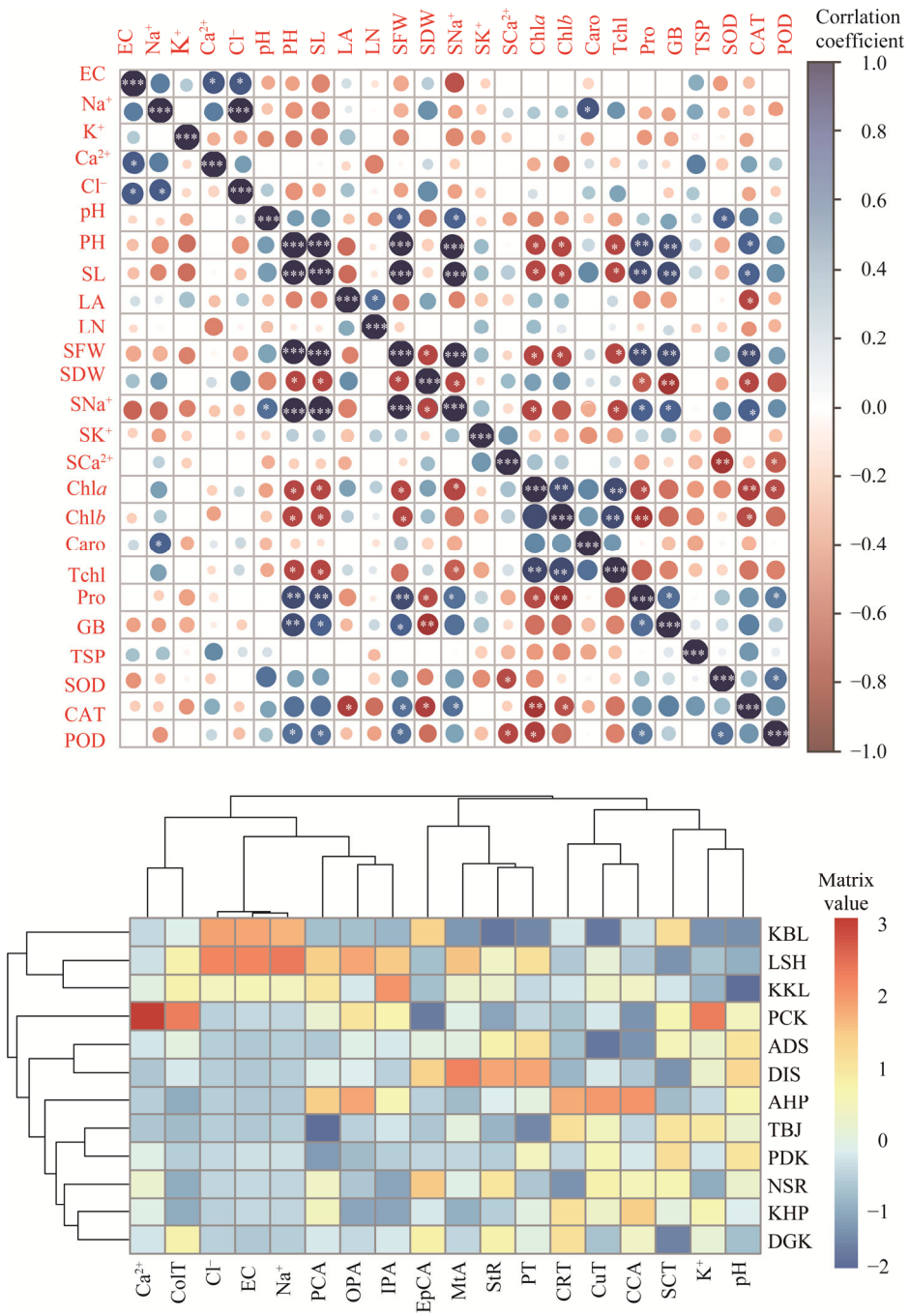

Fig. 8 (a), correlation among soil physical-chemical traits and leaf structural attributes; (b), cluster heatmap for soil physical-chemical traits and leaf structural attributes of *Calotropis procera* populations collected from different habitats of the Punjab Province, Pakistan. *, $P<0.05$ level; **, $P<0.01$ level; ***, $P<0.001$ level.

and canal irrigation. According to Tezara et al. (2011) and Rivas et al. (2020), plants showed high photosynthetic rate, stomatal control, and efficient metabolic performance under drought stress condition. Leaves per plant were exceptionally high in DIS, but smaller in size. Large number of narrow leaves may aid in carbon acquisition as well as water use efficiency by controlling transpiration rate (Mutwakil et al., 2017). Fresh and dry biomass production is a good criterion to judge the tolerance potential in plants against abiotic stresses (Zokaee-Khosroshahi et al., 2014). ADS showed the maximum shoot fresh weight, while that TBJ showed the maximum of shoot dry

weight. The robust growth of both populations is a reflection of their complete dominance to respective habitats.

Abiotic stresses like salinity and water logging, high temperature, and irradiance impose substantial changes in tissues ionic contents, photosynthetic pigments, organic osmolyte level, and antioxidants in plants (Hasanuzzaman et al., 2020). Accumulation of high Na^+ concentration in tissues has been reported in various glycophytes and halophytes (Sekmen et al., 2013), as recorded in LSH population in this study. These plants utilize such ions to maintain the cell osmotic potential and osmoregulatory process under osmotic stress condition (Rouached et al., 2010). Remarkable concentration of shoot K^+ and Ca^{2+} in NSR population showed soil enrichment of these ions. In addition, these are beneficial for plants to regulate the cellular osmotica and metabolic process (Alzahrani et al., 2019). Much higher concentration of photosynthetic pigments (chl*a*, chl*b*, and total chl) was found in AHP population, whereas large quantity of carotenoids was found in DGK population. This increase in pigments seems to be directly associated with photosynthetic efficiency of species under stressful environment (Maimaitiyiming et al., 2017).

Salt tolerant species accumulate bulk amount of organic osmolyte to offset the effects of ROS and free radicals on photosynthetic apparatus and organelles involved in respiratory process, that ultimately lead to the oxidative stress. Osmoprotectants also maintain the protein structure, membrane integrity, and osmotic events in plants (Muchate et al., 2016). In our results, the populations from salt affected lands (LSH, KBL, and KKL) were rated as more tolerant due to the maximum accumulation of proline, GB, and soluble proteins. Plants generally evolve antioxidants mechanism (enzymatic and non-enzymatic) to mitigate and detoxify the effects of ROS. Enzymatic antioxidants like SOD, CAT, and POD, are designed in chain reaction to eliminate and scavenge the superoxide and H_2O_2 in plants (Sheikh-Mohamadi et al., 2017). In current study, all the populations showed different level of antioxidant metabolism with respect to prevailing stress conditions, while the population inhabiting in saline environment (LSH, KBL, and KKL) surpassed in antioxidant activity. Keeping the high level of antioxidants might supplement for salinity or drought stress tolerance by improving the protective strategy against oxidative stress (Zhang et al., 2013).

Hameed et al. (2012) found that desert plants were adapted to limited water availability, therefore, the impact of water stress was not severe as on the other habitat with high moisture availability, especially in tolerant species. The response of differently adapted populations of *C. procera* was very specific, indicating their capability to survive in desert environment. All the populations showed great diversity in stem anatomical tissues like dermal, mechanical, vascular, and storage tissues. The population growing in desert and semi-desert environment showed the maximum stem anatomical parameters, i.e., cuticle thickness, cortical region thickness, cortical cell area, outer phloem area, and pith cell area in AHP population; and stem radius, pith region thickness, and metaxylem area in DIS population. Desert plants modify their structural and functional features to cope with multiple abiotic stresses and successfully survive in such voracious climatic conditions. In earlier studies, cuticle or epidermis thickness is reported as first line of defense in arid plants to minimize the water loss under water scarce conditions (Liu et al., 2020). Another adaptation in these plants is the formation of enlarged stem area due to deposition of storage parenchyma and large vascular bundles. This may certainly aid in water conservation in plant tissues and hence survive with subject to prolonged dry weather condition and low moisture contents (Su et al., 2019). Therefore, AHP population showed enormous succulence in form of storage parenchyma (cortex) to survive under such environment. The formation of large phloem region is another principle strategy of this population that may enhance photosynthetic translocation and partitioning to other parts (Hussain et al., 2021).

Vascular bundles with large metaxylem vessels play a key role in efficient translocation of water and minerals. Tissue sclerification is a prominent feature of plants surviving under saline and drought stress conditions (Hameed et al., 2020). Same result was observed in stem of KBL and NSR populations. Tissue sclerification gives mechanical strength to metabolically active

tissues in order to protect from collapse and desiccations, when water has become vital commodity for plants either due to low soil water potential or low water table (Abd Elhalim et al., 2016). Thick collenchyma layer formed under epidermis and around the cortical tissues is very critical feature of PCK population, which might be their habitat friendly behavior or strategy to overcome the prevailing stress. Collenchyma acts as supporting tissue in plants of dry environment by preventing water loss from surface (Iqbal et al., 2021).

Leaves are quite responsive to climatic conditions, because they are directly exposed to environmental stress (Drake et al., 2019). Leaf thickness showed very differential response to varied environmental conditions, i.e., the populations growing in desert regions showed very thick leaves regarding lamina (AHP) and midrib thickness (DIS and KHP). Leaf thickness might be the result of increased storage parenchyma region to store additional water. This is a critical adaption of desert dwelling species to cope with severe drought condition (Grubb et al., 2015). In addition to thick epidermis and cuticle, trichome size and number, stomatal size, shape, orientation, and regulation are also vital for plants to survive under dry environment. Stomata are generally oriented on abaxial side of leaves in most of desert species, to reduce transpiration rate, especially when leaves are directly subjected to sun rays (Silva et al., 2014). Similar result was observed in AHP population, having more stomata on leaf abaxial surface of plants. Moreover, small size stomata show efficient translocation as compared with larger ones due to low need of water for turgor maintenance (Rudall et al., 2013).

Intensive sclerification around cortical and vascular region of KBL population, hence making leaves stiffer and more fibrous. Cuticle thickening in this population additionally contributes in leaf stiffness, moreover, it also protects from solar irradiance and pathogens infection (Akcin et al., 2015). Large metaxylem formed in leaves of KKL population might be adaptability in order to maintain water supply under low soil water potential. Trichomes act as insulating agent to high wind pressure, rain splashes, and high temperature. These are ecologically important for species of dry environment, which maintain the maximum humidity on surface of leaves (Dolatabadian et al., 2011). Few and large trichomes in PCK population indicate its tolerance and strategy to make sure its survival under limited water supply. ADS population growing along the river/canal bank possessed large stomata on adaxial leaf surface. As stomata are vital for transpiration and gaseous exchange in plants, its opening allow the maximum water utilization along with carbon sequestration. They maintain the plant's vigor and vitality by producing more energy in saturated environmental conditions (Buckley, 2019).

5 Conclusions

It is concluded that survival responses in *C. procera* populations appeared as the result of complex and differential reactions to prevailing stress conditions. The maximum modulation of growth, photosynthetic, and anatomical features in DIS and AHP populations strongly favored in their life cycle completion, and also indicated its tolerance potential under harsh environment. The population inhabiting saline areas showed enhanced level of metabolites and antioxidant to cope with osmotic stress condition. Accumulation of beneficial ions (K^+ and Ca^{2+}) in NSR population and the maximum biomass production (shoot fresh and dry weight) in ADS population shows their success in respective habitats. Overall, growth, physio-biochemical, and anatomical indices observed in these populations are best indicators of their survival and stress tolerance. However, there is a need for further study into the effects of habitats on functional attributes of *C. procera* populations at molecular and genetic levels.

Acknowledgements

I am very grateful to the Ex-Chairman of Botany Department, University of Agriculture, Faisalabad, Pakistan, for providing instruction and platform for computing data and manuscript preparation. In addition, the authors thank reviewers and editors for their helpful comments on improving the quality of this manuscript.

References

Abd Elhalim M E, Abo-Alatta O K, Habib S A, et al. 2016. The anatomical features of the desert halophytes *Zygophyllum album* L. F. and *Nitraria retusa* (Forssk.) Asch. Annals of Agricultural Science, 61(1): 97–104.

Ahanger M A, Tomar N S, Tittal M, et al. 2017. Plant growth under water/salt stress: ROS production, antioxidants and significance of added potassium under such conditions. Physiology and Molecular Biology of Plants, 23(4): 731–744.

Akcin T A, Akcin A, Yalcin E. 2015. Anatomical adaptations to salinity in *Spergularia marina* (Caryophyllaceae) from Turkey. Proceedings of the National Academy of Sciences India Section B: Biological Sciences, 85: 625–634.

Alzahrani S M, Alaraidh I A, Migdadi H, et al. 2019. Physiological, biochemical, and antioxidant properties of two genotypes of *Vicia faba* grown under salinity stress. Pakistan Journal Botany, 51(3): 786–798.

Arnon D I. 1949. Copper enzymes in isolated chloroplasts: Polyphenoloxidase in *Beta vulgaris*. Plant Physiology, 24(1): 1–15.

Bates L S, Waldren R P, Teare I D. 1973. Rapid determination of free proline for water-stress studies. Plant and Soil, 39: 205–207.

Batool A, Ashraf M, Akram N A, et al. 2013. Salt-induced changes in the growth, key physicochemical and biochemical parameters, enzyme activities, and levels of non-enzymatic anti-oxidants in cauliflower (*Brassica oleracea* L.). Journal of Horticultural Science and Biotechnology, 88(2): 231–241.

Boutraa T. 2010. Growth performance and biomass partitioning of the desert shrub *Calotropis procera* under water stress conditions. Journal of Horticultural Science and Biotechnology, 6: 20–26.

Bradford M M. 1976. A rapid and sensitive method for the quantitation of microgram quantities of protein utilizing the principle of protein-dye binding. Analytical Biochemistry, 72(1–2): 248–254.

Buckley T N. 2019. How do stomata respond to water status?. New Phytologist, 224(1): 21–36.

Chance B, Maehly A C. 1955. The assay of catalases and peroxidases. In: David G. Method of Biochemical Analysis. New York: Interscience Publishers Inc., 764–775.

De Faria A P, Marabesi M A, Gaspar M, et al. 2018. The increase of current atmospheric CO_2 and temperature can benefit leaf gas exchanges, carbohydrate content and growth in C_4 grass invaders of the Cerrado biome. Plant Physiology and Biochemistry, 127: 608–616.

Dolatabadian A, Sanavy S A M M, Ghanati F. 2011. Effect of salinity on growth, xylem structure and anatomical characteristics of soybean. Notulae Scientia Biologicae, 3(1): 41–45.

Drake P L, De Boer H J, Schymanski S J, et al. 2019. Two sides to every leaf: water and CO_2 transport in hypostomatous and amphistomatous leaves. New Phytologist, 222(3): 1179–1187.

Duan H, Chaszar B, Lewis J D, et al. 2018. CO_2 and temperature effects on morphological and physiological traits affecting risk of drought-induced mortality. Tree Physiology, 38(8): 1138–1151.

El-Hendawy S E, Hassan W M, Al-Suhaibani N A, et al. 2017. Comparative performance of multivariable agro-physiological parameters for detecting salt tolerance of wheat cultivars under simulated saline field growing conditions. Frontiers of Plant Science, 435: 1–15.

Fatima S, Hameed M, Naz N, et al. 2021. Survival strategies in Khavi grass (*Cymbopogon jwarancusa* (Jones) Schult.) colonizing hot hypersaline and arid environments. Water, Air and Soil Pollution, 232: 1–17.

Giannopolitis C N, Ries S K. 1977. Superoxide dismutases: I. Occurrence in higher plants. Plant Physiology, 59(2): 309–314.

Grieve C M, Grattan S R. 1983. Rapid assay for determination of water-soluble quaternary ammonium compounds. Plant and Soil, 70: 303–307.

Grubb P J, Marañón T, Pugnaire F I, et al. 2015. Relationships between specific leaf area and leaf composition in succulent and non-succulent species of contrasting semi-desert communities in south-eastern Spain. Jounal of Arid Environment, 118: 69–83.

Hameed M, Batool S, Naz N, et al. 2012. Leaf structural modifications for drought tolerance in some differentially adapted ecotypes of blue panic (*Panicum antidotale* Retz.). Acta Physiologiae Plantarum, 34: 1479–1491.

Hameed M, Fatima S, Shah S M, et al. 2020. Ultrastructural response of wheat (*Triticum aestivum* L.) lines to potential allelopathy of *Alstonia scholaris* (L.) R. Br. leaf extract. Turkish Journal of Botany, 44(5): 509–525.

Hasanuzzaman M, Bhuyan M H M, Zulfiqar F, et al. 2020. Reactive oxygen species and antioxidant defense in plants under abiotic stress: Revisiting the crucial role of a universal defense regulator. Antioxidants, 9(8): 681, doi: 10.3390/antiox9080681.

Hassan L M, Galal T M, Farahat E A, et al. 2015. The biology of *Calotropis procera* (Aiton) W. T. Trees, 29: 311–320.

Hussain S, Hussain S, Ali B, et al. 2021. Recent progress in understanding salinity tolerance in plants: Story of Na^+/K^+ balance and beyond. Plant Physiology and Biochemistry, 160: 239–256.

Iqbal U, Hameed M, Ahmad F. 2021. Water conservation strategies through anatomical traits in the endangered arid zone species *Salvadora oleoides* Decne. Turkish Journal of Botany, 45(2): 140–157.

Kaleem M, Hameed M. 2021. Plasticity in structural and functional traits associated with photosynthesis in *Fimbristylis complanata* (Retz.) Link. under salt stress. Pakistan Journal of Botany, 53(4): 1199–1208.

Khan S A, Ranjha M H, Khan A A, et al. 2019. Insecticidal efficacy of wild medicinal plants, *Dhatura alba* and *Calotropis procera*, against *Trogoderma granarium* (Everts) in wheat store grains. Pakistan Journal of Zoology, 51(1): 289–294.

Koutroulis A G. 2019. Dryland changes under different levels of global warming. Science of the Total Environment, 655: 482–511.

Liu C, Li Y, Zhang J, et al. 2020. Optimal community assembly related to leaf economic-hydraulic-anatomical traits. Frontiers of Plant Science, 11: 341, doi: 10.3389/fpls.2020.00341.

Maimaitiyiming M, Ghulam A, Bozzolo A, et al. 2017. Early detection of plant physiological responses to different levels of water stress using reflectance spectroscopy. Remote Sensing of Environment, 9(7): 745, doi: 10.3390/rs9070745.

Menge E O, Stobo-Wilson A, Oliveira S L, et al. 2016. The potential distribution of the woody weed *Calotropis procera* (Aiton) WT Aiton (Asclepiadaceae) in Australia. The Rangeland Journal, 38(1): 35–46.

Muchate N S, Nikalje G C, Rajurkar N S, et al. 2016. Physiological responses of the halophyte *Sesuvium portulacastrum* to salt stress and their relevance for saline soil bio-reclamation. Flora. 224: 96–105.

Muhammad I, Shalmani A, Ali M, et al. 2021. Mechanisms regulating the dynamics of photosynthesis under abiotic stresses. Frontiers of Plant Science, 11: 615942, doi: 10.3389/fpls.2020.615942.

Mutwakil M Z, Hajrah N H, Atef A, et al. 2017. Transcriptomic and metabolic responses of *Calotropis procera* to salt and drought stress. BMC Plant Biology, 17(1): 231, doi: 10.1186/s12870-017-1155-7.

Obidiegwu J E, Bryan G J, Jones H G, et al. 2015. Coping with drought: Stress and adaptive responses in potato and perspectives for improvement. Frontiers of Plant Science, 6: 542, doi: 10.3389/fpls.2015.00542.

Paccard A, Vance M, Willi Y. 2013. Weak impact of fine-scale landscape heterogeneity on evolutionary potential in *Arabidopsis lyrata*. Journal of Evolutionary Biology 26(11): 2331–2340.

Peñuelas J, Sardans J, Filella I, et al. 2018. Assessment of the impacts of climate change on Mediterranean terrestrial ecosystems based on data from field experiments and long-term monitored field gradients in Catalonia. Environmental and Experimental Botany, 152: 49–59.

Pompelli M F, Mendes K R, Ramos M V, et al. 2019. Mesophyll thickness and sclerophylly among *Calotropis procera* morphotypes reveal water-saved adaptation to environments. Journal of Arid Land, 11(6): 795–810.

R Development Core Team. 2017. R: A Language and Environment for Statistical Computing R Foundation for Statistical Computing, Vienna, Austria. [2022-01-15]. http://www.R-project.org.

Rivas R, Barros V, Falcão H, et al. 2020. Ecophysiological traits of invasive C_3 species *Calotropis procera* to maintain high photosynthetic performance under high VPD and low soil water balance in semi-arid and seacoast zones. Frontiers of Plant Science, 11: 717, doi: 10.3389/fpls.2020.00717.

Rouached H, Secco D, Arpat B A. 2010. Regulation of ion homeostasis in plants: Current approaches and future challenges. Plant Signaling and Behavior, 5(5): 501–502.

Rudall P J, Hilton J, Bateman R M. 2013. Several developmental and morphogenetic factors govern the evolution of stomatal patterning in land plants. New Phytologist, 200(3): 598–614.

Ruzin S E. 1999. Plant Microtechnique and Microscopy. New York: Oxford University Press, 198.

Sachdev S, Ansari S A, Ansari M I, et al. 2021. Abiotic stress and reactive oxygen species: Generation, signaling, and defense mechanisms. Antioxidants, 10(2): 277, doi: 10.3390/antiox10020277.

Sekmen A H, Bor M, Ozdemir F, et al. 2013. Current concepts about salinity and salinity tolerance in plants. Climate Change and Plant Abiotic Stress Tolerance, 28: 163–188.

Sheikh-Mohamadi M H, Etemadi N, Nikbakht A, et al. 2017. Antioxidant defence system and physiological responses of Iranian crested wheatgrass (*Agropyron cristatum* L.) to drought and salinity stress. Acta Physiologiae Plantarum, 39(11): 245, doi: 10.1007/s11738-017-2543-1.

Silva H, Sagardia S, Ortiz M, et al. 2014. Relationships between leaf anatomy, morphology, and water use efficiency in *Aloe vera* (L) Burm f. as a function of water availability. Revista Chilena de Historia Natural, 87: 13, doi: 10.1186/s40693-014-0013-3.

Snedecor G W, Cochran W G. 1980. Statistical Methods (7th ed.). Ames: Iowa State University Press, 68–93.

Steel R G D, Torrie J H, Dicky D A. 1997. Principles and Procedures of Statistics: A Biometrical Approach. New York: McGraw Hill Inc., 25–68.

Su R, Zhou R, Mmadi M A, et al. 2019. Root diversity in sesame (*Sesamum indicum* L.): Insights into the morphological, anatomical and gene expression profiles. Planta, 250(5): 1461–1474.

Tezara W, Colombo R, Coronel I, et al. 2011. Water relations and photosynthetic capacity of two species of *Calotropis* in a tropical semi-arid ecosystem. Annals of Botany, 107(3): 397–405.

Wolf B. 1982. An improved universal extracting solution and its use for diagnosing soil fertility. Communications in Soil Science and Plant Analysis, 13(12): 1005–1033.

Zhang W, Tian Z, Pan X, et al. 2013. Oxidative stress and non-enzymatic antioxidants in leaves of three edible canna cultivars under drought stress. Horticulture, Environment, and Biotechnology, 54(1): 1–8.

Zokaee-Khosroshahi M, Esna-Ashari M, Ershadi A, et al. 2014. Morphological changes in response to drought stress in cultivated and wild almond species. International Journal of Horticultural Science, 1(1): 79–92.